Chemical Engineering Journal 448 (2022) 137615

Contents lists available at ScienceDirect

Chemical Engineering Journal

journal homepage: www.elsevier.com/locate/cej

Long-term performance of highly selective carbon hollow fiber membranes for biogas upgrading in the presence of H_2S and water vapor

Adele Brunetti [a,*,1], Linfeng Lei [b,1], Elisa Avruscio [a], Dionysis S. Karousos [c,*], Arne Lindbråthen [d], Evangelos P. Kouvelos [c], Xuezhong He [e,*], Evangelos P. Favvas [c,*], Giuseppe Barbieri [a]

[a] National Research Council - Institute on Membrane Technology (ITM–CNR), Via Pietro BUCCI, cubo 17C, 87036 Rende, CS, Italy
[b] State Key Laboratory of Chemical Engineering, School of Chemical Engineering, East China University of Science and Technology, 130 Meilong Road, Shanghai 200237, China
[c] Institute of Nanoscience and Nanotechnology, National Center for Scientific Research "Demokritos", Aghia Paraskevi 153 41, Athens, Greece
[d] Department of Chemical Engineering, Norwegian University of Science and Technology, NO-7491 Trondheim, Norway
[e] Department of Chemical Engineering, Guangdong Technion-Israel Institute of Technology (GTIIT), 241 Daxue Road, Shantou 515063, China

ARTICLE INFO

Keywords:
Biogas upgrading
Carbon capture
Carbon hollow fiber membranes
H_2S
CO_2/CH_4 selectivity
Gas sorption

ABSTRACT

Biogas is an increasingly attractive renewable resource that needs to be upgraded to meet either the natural gas pipeline quality or the biomethane requirement. The use of carbon membranes is a promising alternative to conventional separation technologies, but, up to now, few attempts have been made to systematically investigate their separation performance under real biogas upgrading conditions, for instance, the presence of water vapor and H_2S in the feed stream.

In this work, for the first time in literature, the separation performances of as-prepared cellulose-based carbon hollow fiber membranes were monitored for 183 days under continuous exposure to a gas stream also containing H_2S and/or water vapor. After the evaluation of their CO_2 and CH_4 sorption (2,98 mmol g^{-1} and 2,00 mmol g^{-1}, respectively at 298 K and 10 bar), diffusion(2.45×10^{-7} cm^2 s^{-1} for CO_2), and permeation properties (120.9 and 2.3 barrer, respectively at 308 K) with single gases, long-term tests were carried out by feeding gas mixtures with typical biogas composition. It was found that the exposure of the membranes to H_2S (up to 500 ppm) and water vapor (relative humidity of 90%) provoked a reduction of CO_2 and CH_4 permeability compared to the "clean and dry" mixed gas, which resulted in an increment of selectivity, which reached a value of more than 200. Overall, after more than 180 days of continuous testing, the membranes exhibited remarkable CO_2/CH_4 selectivity with endurability of the H_2S and water vapor, confirming the fact of being good candidates for biogas upgrading.

1. Introduction

Natural gas, a cleaner energy resource compared to coal and petroleum, has been thought as an attractive option to evade excessive CO_2 emissions. As projected by the International Energy Agency (IEA) in the "Net Zero by 2050" report, the global natural gas demand will increase expeditiously, from 3900 billion cubic meters in 2020 to 4600 and 5700 in 2030 and 2050, respectively [1]. Nevertheless, owing to its non-renewable inherent quality, natural gas is still far from being a perfect long-term energy solution [2]. Production of energy resources from biomass could be a promising approach reducing CO_2 emissions and to fight against global climate change. Biogas, which is normally produced from the anaerobic digestion of organic wastes in landfills, agricultural residues, and industrial/municipal wastes, is one of the most common and commercially available renewable energy resources [2,3]. The production of biogas not only provides a practical solution for transferring biowastes to an energy resource but also avoids the CO_2 and CH_4 (whose greenhouse effect is 25 times stronger than CO_2) emissions to the atmosphere. In general, the collected raw biogas mainly contains 35–70% CH_4, 30%-65% CO_2, associated with water vapor, N_2, hydrogen sulfide and trace amounts of volatile organic compounds [2,4]. Upgrading biogas is mainly to remove CO_2 from the raw streams, in order to meet the quality standards of natural gas grids.

* Corresponding authors.
E-mail addresses: adele.brunetti@cnr.it (A. Brunetti), d.karousos@inn.demokritos.gr (D.S. Karousos), xuezhong.he@gtiit.edu.cn (X. He), e.favvas@inn.demokritos.gr (E.P. Favvas).
[1] These authors contributed equally.

https://doi.org/10.1016/j.cej.2022.137615
Received 14 March 2022; Received in revised form 1 June 2022; Accepted 16 June 2022
Available online 18 June 2022

Nomenclature

symbols

b(Toth & Sips)	Parameter of Toth and Sips equations
b_i with i from 0 to 4	Virial coefficients
$C(t)$	Gas concentration at spherical particle surface at time t
C_∞	Gas concentration at spherical particle surface after infinite time
D	Diffusivity time constant
D_{iorj}	Diffusivity coefficient of compound i or j
m_t	Adsorbed mass at time t
m_∞	Adsorbed mass at infinite time
q	Adsorption capacity
q_m	Parameter of Toth and Sips equations
P	Pressure
P_i	Partial pressure of gas i
P_i^{Feed}	Partial pressure of gas i *in feed stream*
$P_i^{Retentate}$	Partial pressure of gas i *in retentate stream*
P_i^{Sweep}	Partial pressure of gas i *in sweep stream*
R	Universal gas constant
S_{iorj}	Solubility coefficient of compound i or j
t	Time
t(Toth & Sips)	Parameter of Toth and Sips equations
T	Temperature

Greek symbols

α_i with i from 0 to 2	Virial coefficients
α	Adsorbent spherical particle radius
ΔH_{ads}	Enthalpy of adsorption
ΔP_i	Partial pressure difference of i-specie

Acronyms

CHFMs	carbon hollow fiber membranes

Membrane-based biogas upgrading that is mainly CO_2/CH_4 separation, is considered a promising technology compared to conventional separation processes, such as amine and water scrubbing, owing to its advantages of environmental-friendliness, small footprint, energy-saving through low operational costs, and process flexibility. However, commercially available polymeric membranes, such as cellulose acetate, normally suffer from materials-related limitations, such as plasticization [5] and Robeson's upper bound limit [6]. Thus, there is still a strong need to develop advanced membranes which are robust, high-performing, as well as cost-effective. Besides, it is also noteworthy to emphasize that the membranes with water vapor and H_2S endurability are highly desired for biogas upgrading since those impurities often exist in the raw streams. Carbon membranes have shown their high potential for the application in biogas upgrading [7-11]. A pilot multi-module carbon membrane system for real biogas upgrading was constructed by MemfoACT (a Norwegian company that closed in 2014). The multi-module system comprised of 24 membrane modules (each module contained 2000 carbon hollow fibers) was tested at 15–20 °C and 20 bar with a 10 Nm^3/h feed flow rate (63 mol.% CH_4, 1 ppm H_2S, balance CO_2) [10,11]. It was reported that a single-stage pilot system could reach a CH_4 purity of 96 %mol at a CH_4 recovery of over 98% [11]. However, these reported carbon hollow fiber membranes were made from cellulose acetate exhibiting variations of separation properties under water vapor and H_2S exposure. In this case, when a small membrane module was dynamically exposed to a humidified biogas stream, CO_2 permeance dropped by 60% while CO_2/CH_4 selectivity increased four times [10]. And when the cellulose acetate-based carbon membranes were exposed to H_2S, it was found that the CO_2 permeability lost about 70 %.[12]. To realize the real industrial application for biogas upgrading using carbon membranes, it is necessary to develop carbon membranes in a more robust structure to restrain the performance fluctuation. Cellulose-derived carbon membranes showed good separation performance at different transmembrane pressure differences, temperatures, and feed gas compositions [13]. The material testing and techno-economic feasibility analysis that carbon membranes have great potential for CO_2/CH_4 separations. However, in order to bring the technology to future industrial applications (e.g., biogas), testing such membranes in a simulated environment (e.g., with the existence of H_2S and water vapor) is crucial to document the long-term stability.

Recently, similar carbon membranes have shown relatively stable permeation for testing gases in presence of water vapor, because of the high hydrophilicity of those carbon membranes that could allow water vapor to permeate through the membrane easily.[14-16]. For instance, a permeation test under a mixed gas saturated with water vapor at 90 °C for carbon hollow fiber membranes showed good stability over 200 h [15].

Yet, few attempts have been made to systematically investigate the separation performance of carbon membranes under an H_2S exposure condition. Since carbon molecular sieve membranes have a rigid structure, their pore structure can be maintained under some harsh conditions, such as high operation pressure over 100 bar and high operation temperature over 200 °C [37]. Thus, it can be expected that there will not be any significant structural change under these testing conditions. However, H_2S is expected to behave similarly to water vapour. Therefore, we expected that water vapor and H_2S will permeate through the reported carbon membranes, and will not cause a significant pore blockage, and the adsorbed H_2S and water vapor can be partially removed by thermal regeneration. Anyway, some additional investigation should be further carried out to document the water and H_2S adsorption inside the cellulose-based carbon membranes.

In this work, long-term tests for cellulose-based hollow fiber membranes were carried out under harsh feeding conditions with high relative humidity (RH) of 90 % and a high content of H_2S (up to 500 ppm), which are close to the industrial biogas streams. Initially, the sorption and diffusion of CO_2 and CH_4 in the as-prepared membranes were evaluated to provide indications about the transport mechanism governing the permeation of the two main species. Subsequently, the membrane module underwent 183 days of continuous testing under the exposure of gas mixtures containing H_2S or/and water vapor, without being damaged or losing its capability to separate the CO_2/CH_4 mixture. Permeability and selectivity differences measured under mixed-gas conditions were systematically analyzed to clarify the different mass transport properties that gases exhibit under mixed-gas conditions as well as in presence of species such as water vapour or H_2S.

2. Materials and methods

2.1. Membrane preparation

The carbon hollow fiber membranes developed in this work were prepared from cellulose hollow fiber precursors. A detailed description of the membrane preparation method can be found in our previous work [13,15,17,18]. In brief, the cellulose hollow fiber precursors were fabricated by a dry-wet spinning process. During the spinning, a dope solution was composed of 12 wt% microcrystalline cellulose (Advice PH-101) and 88 wt% co-solvent (1-Ethyl-3-methylimidazolium Acetate and dimethyl sulfoxide with a weight ratio of 3:1), while a bore solution consists of 80 wt% cosolvent and 20 wt% non-solvent of water. The as-spun fresh hollow fibers were then washed in a water bath for 72 h to remove residual solvents (during that time the water was renewed at

least three times), followed subsequently by a solvent exchange procedure that hollow fibers were immersed in a 10 wt% glycerol aqueous solution for 48 h. The obtained cellulose hollow fibers were dried at room temperature for 12 h. Afterward, the precursors were carbonized with an argon purge gas using the carbonization procedure described elsewhere [19]. The carbon membrane presented a symmetric structure with a thickness of 30–40 μm as shown in Figure S1,a-d. They show a smooth surface along the fibers (Figure S1e), and present good mechanical flexibility with a bend radius of less than 1.5 cm (Figure S1f). A hollow fiber membrane module containing 5 hollow fibers (having a thickness of 45 μm) for a total membrane area of 9.5 cm^2 was then constructed in a 3/8-inch Swagelok® stainless steel tube sealed by LOCTITE® EA 3430 epoxy adhesive, which was used for the gas permeation and long-term tests. Gas sorption measurements CO_2 and CH_4 adsorption isotherms were measured at 273, 298 and 323 K and pressures up to 20 bar using an Intelligent Gravimetric Analyser (IGA, Hiden Isochema) [19]. The ground carbon hollow fiber membrane sample was outgassed at 523 K overnight, under an ultrahigh vacuum (10^{-7} mbar). The temperature was controlled using a recirculating cooler and buoyancy corrections are applied to mass measurements.

2.2. Single gas isotherm fitting

Ground membrane sample data regression was achieved with the semi-empirical Toth isotherm (Eq. (1)) for CO_2 in the pressure range 0–20 bar for all three temperatures with good agreement with experimental data (R^2 greater than 99.9%).

$$q = q_m \frac{bP}{\left(1 + (bP)^t\right)^{1/t}} \tag{1}$$

On the other hand, optimum (R^2 greater than 99.0%) data regression for CH_4 was achieved with the semi-empirical Sips isotherm (Eq. (2)) between 0 and 20 bar at 323 K and in the restricted pressure range of 0–14 bar at 273 and 298 K.

$$q = q_m \frac{(bP)^{1/t}}{1 + (bP)^{1/t}} \tag{2}$$

Three-parameter isotherm models [20] were selected for a more accurate fitting of experimental data in both the low and the high-pressure range. CO_2 isotherms were of type II at all three temperatures and the low declination from the theoretical Langmuir model, allowed the use of the Toth model, which considers a quasi-Gaussian distribution of heats of adsorption for different active sites. CH_4 isotherms declined more than CO_2 from the Langmuir model, in particular for lower temperatures and higher pressures. Therefore, the Sips model was used, since it assimilates the Freundlich model's increase of adsorbed amount at higher pressures, without declining considerably from Henry's law at low pressures.

2.3. The heat of adsorption calculation for activated carbon

Virial equation (Eq. (3)) was used for regression of single gas adsorption data on activated carbon:

$$lnP = \left(\alpha_0 + \alpha_1 q + \alpha_2 q^2\right) + \left(b_0 + b_1 q + b_2 q^2 + b_3 q^3 + b_4 q^4\right)\frac{1}{T} + lnq \tag{3}$$

Since $\Delta H_{ads} = R \bullet \left(\frac{d(lnP)}{d(1/T)}\right)_q$ is the differential isosteric enthalpy of adsorption, the respective isosteric heat of adsorption was then calculated from Eq. (4):

$$-\Delta H_{ads} = -R\left(b_0 + b_1 q + b_2 q^2 + b_3 q^3 + b_4 q^4\right) \tag{4}$$

Furthermore, the kinetic adsorption for CO_2 was calculated by using the following equation [21]:

$$\frac{m_t}{m_\infty} = 1 - \frac{3D}{b} exp(-bt)\left[1 - \frac{\sqrt{\frac{b}{D}}}{\tan\sqrt{\frac{b}{D}}}\right] + \frac{6b}{\pi^2 D}\sum_{j=1}^{\infty}\left[\frac{exp\left(-Dj^2\pi^2 t\right)}{j^2\left(j^2\pi^2 - \frac{b}{D}\right)}\right] \tag{5}$$

where the adsorbent particle is considered to be a sphere of radius α and m_t, m_∞ are the adsorbed gas amount at time t and ∞, respectively, whereas D is the diffusion time constant, i.e.,:

$$D = \frac{Diffusivity}{\alpha^2} \tag{6}$$

When pressure steps are rather ramping than step changes with time and the gas adsorbs very fast, it is considered that the adsorbate concentration at the external surface of the adsorbent particle follows a gradual exponential increase with time (Eq. (7)).

$$C(t) = C_\infty(1 - exp(-bt)) \tag{7}$$

2.4. Mass transport properties evaluation

The mass transport properties of the carbon-based membrane module were measured at 308 K up to 9.6 bar for CO_2, N_2, and CH_4 as single gases and a CO_2:CH_4 binary mixture with and without H_2S at 9.6 bar (Table 1), also in presence of water vapor. The choice of temperature and feed pressure was done considering the typical conditions for biogas upgrading and grid injection. Fig. 1 shows the experimental apparatus used for carrying out the gas permeation experiments. The membrane module was placed in a furnace for controlling the temperature and it was fed with the gases (single and in mixture) using mass flow controllers (Brooks Instruments 5850S) to tune the feed flow rates. Gas mixtures were already prepared in certified bottles, as well as single gases whose purity was above 4.5. The feed pressure was controlled with a back-pressure regulator (Swagelok KBP series) on the retentate line, two pressure gauges were installed on the feed and retentate confirming the absence of appreciable pressure drop along this line. To provide humidified gases, the upstream was fed into a humidifier placed before the membrane module, held at the same temperature and pressure as the membrane, to assure stream saturation. Three humidity sensors (Digitron HLX31PFTE) on the feed, retentate, and permeate lines, respectively were used to measure the relative humidity of these streams during the long-time measurements. A constant sweep gas was applied during the experiments and permeate pressure was maintained at atmospheric value during single gas measurements. Nevertheless, a slightly higher permeate pressure was measured in the case of the mixture owing to the pressure drop in the passage of the gas stream through the micro-gas-chromatograph.

The membrane module was exposed to a gas stream at all times; nitrogen was fed into the module to maintain a transmembrane pressure difference of 9.6 bar when no experiment was being performed. Prior to

Table 1
Operating conditions used in the experimental measurements.

Temperature (K)	308
Feed pressure (bar)	9.6 (for mixtures) 5–9 (for single gas)
Permeate pressure (bar)	1.03–1.2 (for mixtures)1 (for single gas)
Relative humidity (%)	0–95
Single gases	CO_2, N_2, CH_4
Mixtures composition (molar ratio)	1 – CO_2: CH_4 = 39.8:60.2 2 - CO_2: CH_4: N_2 = 37.35:56.95:5.69 + 203 ppm of H_2S 3 – N_2:H_2S = 99.9538 + 462 ppm of H_2S
Sweep gas (mL(STP) min^{-1})	5 (N_2)
Feed flow rates (mL(STP) min^{-1})	300–500
Reference operating conditions during stand-by periods	under N_2 flow at 9.6 bar as feed pressure and 308 K

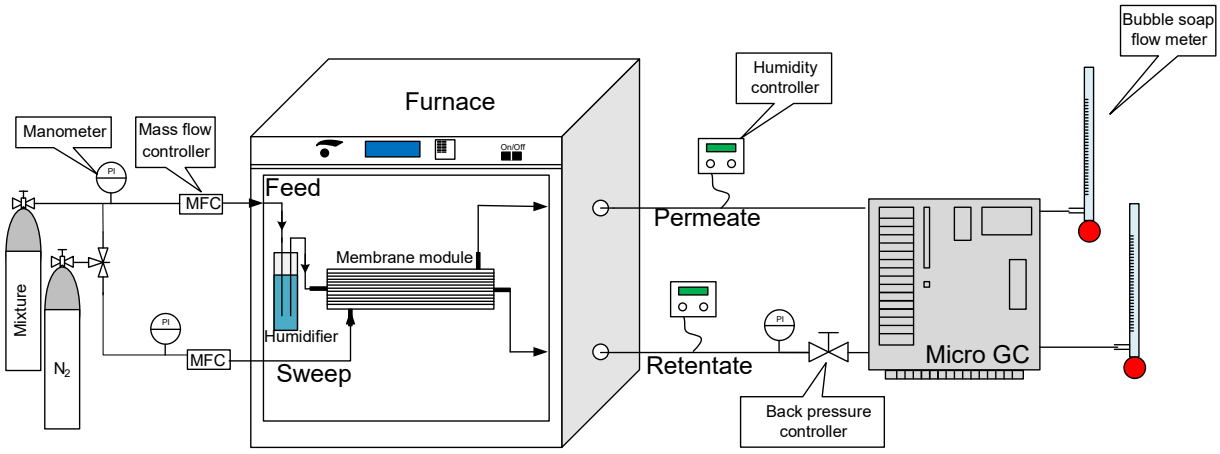

Fig. 1. Experimental setup for the gas permeation measurements.

any change in the feed gas type, the module was opportunely "washed" by feeding the gas of interest for 30 min before measurement. Most of the results reported in this work are obtained with a standard deviation below 5 %. Error bars are shown in the figures only when the error is above this value.

A micro gas chromatograph (Agilent 990) with three modules each one equipped with a different chromatographic column (MolSieve 5 Å, PoraPLOT Q, CP-Sil 19 CB) and three TCD was used for analyzing retentate and permeate streams. Two temperature sensors located at the ends of the membrane module measured the temperature.

The separation properties of the membrane were evaluated in terms of permeance, permeability, and selectivity. Permeance is the ratio of permeating flux and the partial pressure differences between the two membrane sides (Eq. 8), permeability was then calculated as the product of permeance and the membrane thickness (Eq. (9)):

$$Permeance_i = \frac{Permeating\ flux_i}{\Delta P_i},\ GPU \tag{8}$$

$$Permeability_i = Permeance_i \times Membrane\ thickness,\ barrer \tag{9}$$

All the measurements were carried out with a stage-cut of lower than 1%; therefore, the partial pressure profiles in the two membrane sides were negligible and we calculated the driving force by using Eq. (10).

$$\overline{\Delta P_i} = \left[\left(\frac{P_i^{Feed} + P_i^{Retentate}}{2}\right) - \left(\frac{P_i^{Permeate} + P_i^{Sweep}}{2}\right)\right],\ Pa \tag{10}$$

The ratio between the permeability of a gas pair is the selectivity (Eq. (11)).

$$Selectivity_{ij} = \frac{Permeability_i}{Permeability_j},\ - \tag{11}$$

Selectivity based on single gas experiments was calculated by the gas permeability measured by separately feeding to the membrane single gases. The "actual" selectivity was evaluated by the gas permeability of the two gases measured feeding a gas mixture. We will indicate "selectivity" as the one measured feeding a gas mixture and "single gas selectivity" as the other one (Eq. (11)). The permeability is the product of solubility and diffusivity coefficients (Eq.12), therefore, the selectivity can be written also as (Eq. (13)):

$$Permeability_i = S_i D_i \tag{12}$$

$$Selectivityi/j = \left(\frac{S_i}{S_j}\right)\left(\frac{D_i}{D_j}\right) \tag{13}$$

where, $\frac{D_i}{D_j}$ is the diffusion selectivity and $\frac{S_i}{S_j}$ is the sorption selectivity.

The difference in the permeability of each gas measured during the long-term tests at different feeding conditions with respect to the one measured as a single gas at a reference time was calculated by Eq. (14). An analogous relation was defined in terms of ratio (Eq. (15)) for evaluating the deviation of the selectivity concerning the single gas one measured at a reference time (e.g., at t = 0, after H_2S exposure; after H_2O vapor exposure).

$$Permeability\ difference = \frac{Permeability_i\big|_{t=t_1} - Permeability_i^{Single\ gas}\big|_{t=t_{reference}}}{Permeability_i^{Single\ gas}\big|_{t=t_{reference}}} \tag{14}$$

$$Selectivity\ ratio = \frac{Selectivity_i\big|_{t=t_1}}{Selectivity_{i,j}^{Single\ gas}\big|_{t=t_{reference}}} \tag{15}$$

3. Results and discussion

3.1. Gas sorption

An important aspect in the evaluation of the mass transport properties of membranes is played by the sorption and the diffusion in the membrane bulk. For this purpose, we performed single gas sorption isotherms to evaluate the sorption mechanism of the two investigated gases. The sorption isotherms showed (Fig. 2 – top side) a high affinity to CO_2, which dominated the sorption in the membrane matrix, resulting in a CO_2 concentration higher than that of CH_4 at all the considered temperature values. CH_4 showed a behavior similar to CO_2 but with at least 1/3 lower concentration values of CO_2. More interestingly is that at 273 K the CH_4 adsorption isotherm follows a typical Langmuir-type shape up to about 12 bar, where a step in the isotherm is observed. This behaviour is also observed at 298 K but weaker. This fact can be attributed to the transition of the pore filling region from a shrunken-pore phase to an expanded-pore one, something that has been reported mainly for CO_2 adsorption in MOFs structures [22,23]. The measured isotherms were fitted with the Toth (Eq. (1)) and Sips (Eq. (2)) three parameter isotherm models [21] for CO_2 and CH_4 respectively, which described very well the sorption mechanism of the two gases, especially below 15 bar includes the range of pressure investigated in this work. The regression parameters of fitted isotherms can be found in Table 2.

The measured sorption selectivity of 1.5 at 10 bar and 298 K, is a value very close to the respective literature value [24] that emerges from CO_2 and CH_4 isotherms of ground carbon hollow fiber membranes, derived from P84 co-polyimide hollow fiber precursor pyrolyzed up to 1173 K under N_2 flow. This choice was done owing the lack of data of cellulose based hollow fiber carbon membranes and because the membranes were prepared by the same method and all the adsorption measurements were done in the same instrument. Similar values, of 1.9 at

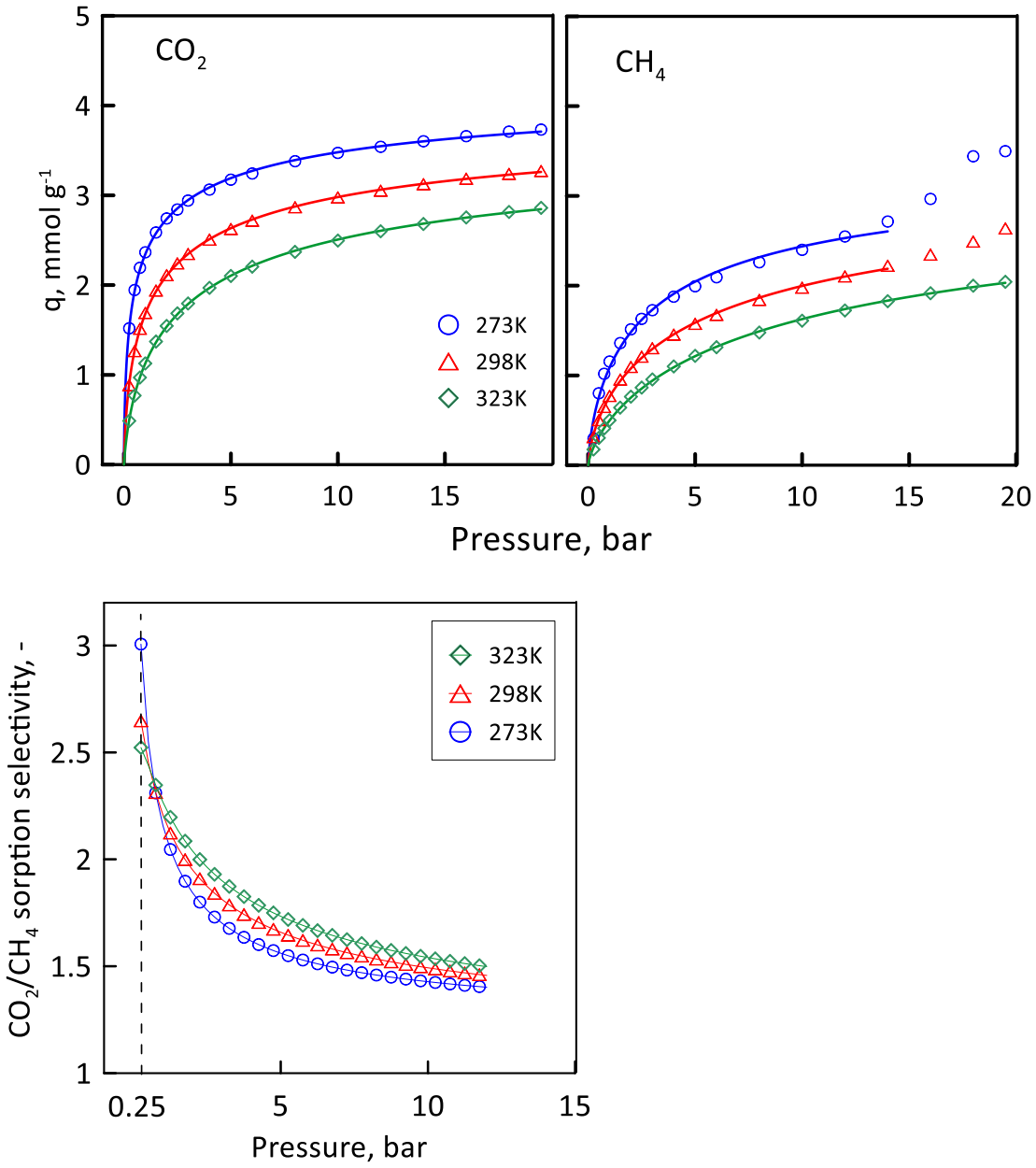

Fig. 2. CO_2 (top left-side) and CH_4 (top right-side) single gas, gravimetric adsorption isotherm (Data fitted by Toth and Sips isotherms for CO_2 and CH_4 respectively); (bottom left-side) sorption CO_2/CH_4 selectivity for carbon membranes adsorbent at 273 K (circles), 298 K (triangles) and 323 K (squares). (See sample CHFM-RT in L. Lei et al. [17] for comparison).

Table 2
Regression parameters of fitted single gas gravimetric isotherm data.

Adsorbent	T [K]	Parameters					
		q_m		b		t	
		CO_2	CH_4	CO_2	CH_4	CO_2	CH_4
Carbon membrane-based sample	273	19.537	3.501	0.054	3.24E-06	0.372	1.416
	298	12.689	3.489	0.032	1.53E-06	0.658	1.470
	323	10.733	3.341	0.015	9.32E-07	1.912	1.362

*Toth fitting in the range 0–2000 kPa for CO_2 and Sips between 0 and 1400 kPa for CH_4.

10 bar and 1.78 a 15 bar, of sorption selectivity at 298 K were measured in our previous work [19]. Also, the adsorption amount of 2.6 mmol/g of CO_2 at 298 K, for a similar material, wood pulp cellulose/ionic liquid-based carbon molecular sieve membrane, is reported in values very close to this work [14].

The low sorption selectivity value can be explained as a consequence of the fact that the CO_2-selective microporous separation layer is only a small mass fraction of the whole ground carbon hollow fiber membrane powder [14,25-28]. A closer look at the three curves presented in Fig. 2 (bottom left-side) also reveals that while at pressures below 1 bar CO_2/CH_4 selectivity becomes higher for lower temperatures, above 1 bar this trend is inversed. Activated adsorption for micropore filling, which is the predominant sorption mechanism at low pressures, can explain this selectivity curve crossover, since the activation energy needed for entering micropores is higher for CH_4 than for CO_2 [29]. In other words, at low pressures the lower the temperature, the fewer adsorption sites

inside micropores become accessible for CH_4, while CO_2 is not affected to the same degree. On the contrary, at pressures above 1 bar higher temperatures favour CO_2, since CH_4 is less strongly physisorbed (smaller heat of adsorption) and desorbs more easily. This is also confirmed by the heat of sorption for both CO_2 and CH_4.

By using the Virial equation (Eq. (3)), the heats of adsorption for both CO_2 and CH_4 gas were calculated (Supplementary Information, Figure S2, Table S1, Table S2) and in the case of CO_2, the diffusion coefficient by means of Eq. (5) was determined. The importance of the heat of adsorption knowledge is based mainly because this property/value is strongly correlated to the kind of sorption phenomenon. If the isosteric heat of adsorption is lower than 80 kJ mol^{-1} then we have physisorption, whereas if this value is between 80 and 200 kJ mol^{-1} the sorption is based on chemical bonding. Of course, the heat of adsorption is affected by the process temperature, the adsorbate, and the nature of the adsorbent surface. As higher the ΔH the stronger the sorption contribution. The heat of adsorption calculated for both gases (39.037 ± 0.325 kJ mol^{-1} and 23.181 ± 0.774 kJ mol^{-1} for CO_2 and CH_4, respectively) confirmed that the physisorption is mainly occurring in the membrane separating layer.

Because pressure steps (Fig. 3) are rather ramping than step changes with time and CO_2 adsorbs very fast, the adsorbate concentration at the external surface of the adsorbent was described with Eq. (7), which, in specific, is used as a boundary condition for the derivation of the equation (5) (see Fig. 3, left-side).

As is shown in Fig. 3 right-side, the pressure ramped from 250 to 500 mbar with time reaching the plateau of 500 mbar at 2.6 s. Taking this into consideration, the derivation of diffusivity time constant from transient adsorption curves shown in Fig. 3 is questionable, since for the fast CO_2 adsorption rate the increase of the adsorbed gas amount may be masked by a slower pressure increase. However, the three transient curves are shown in Fig. 3 (left-side) reach a plateau at times longer than 2.6 s, which in particular for the 273 K curve, makes the possibility of masking more unlikely.

The applicability of the transient curve regression method is validated by a second diffusivity calculation method, based on the assumption that single gas permeability is the product of diffusivity and solubility [30], the latter being calculated here as the slope of the secant at the isotherm point corresponding to the pressure of 2 bar. For these calculations the skeletal density $1.35x10^3$ kg m^{-3} and the CO_2 and CH_4 single gas permeabilities at 2 bar, 298 K were taken from previous work on the same membrane material [19]. Note that the particle size of the ground carbon hollow fiber membrane differs from the sample presented in the previous work [19], which is reflected in corresponding differences of isotherms and finally in the calculated diffusivities [31]. From Eq. (6), the ratio of diffusivity (calculated as "permeability/solubility coefficient") by the diffusion time constant (calculated from regression with Eq. (5)), provided the theoretical radius of the adsorbent particle (Table 3). The value of 14.7 μm which was found is reasonable for a carbon powder produced by grinding the membrane sample.

Furthermore, the value of 4.5×10^{-9} cm^2 s^{-1} for CH_4 diffusivity was calculated as single gas "permeability/sorption coefficient" ratio, at 2 bar and 298 K. However, accurate regression of adsorbed CH_4 transient curves with Eq. (5) could not be achieved.

In the case of our membranes, at the temperature of 298 K, the diffusivities, calculated from sorption measurements, were found to be 2.45×10^{-7} and 4.5×10^{-9} cm^2 s^{-1} for CO_2 and CH_4 respectively, correspondent to a $\left(\frac{D_i}{D_j}\right)$ of about 54,5 while the selectivity calculated from permeation measurements is 53.3 ± 4.7 (Table 3 and Table 4). Consequently, as emerges from Fig. 2 (bottom left side), the sorption selectivity $\left(\frac{S_i}{S_j}\right)$ has a value lower than 1.5 and therefore the contribution of this factor is of second order, confirming that the permeation through the membrane is mainly controlled by diffusion.

Table 3
Parameters derived by kinetic CO_2 adsorption data (regression with Eq. (5)) and diffusivity calculated as single gas "permeability/solubility" ratio, at 2 bar.

Temperature (K)	Diffusion time constant (s^{-1})	Diffusivity (cm^2 s^{-1})	Parameter *b* (s^{-1})	Sorbent particle radius (μm)
273	0.103 ± 1.37E-03	2.23E-07**	0.85 ± 8.41E-03	14.715
298	0.113 ± 6.04E-04	2.45E-07*	1.02 ± 6.39E-03	14.715**
323	0.120 ± 1.03E-03	2.60E-07**	1.11 ± 1.047E-02	14.715

* calculated from single gas permeability/sorption coefficient ratio, at 2 bar.
** resulting from Eq. (6).

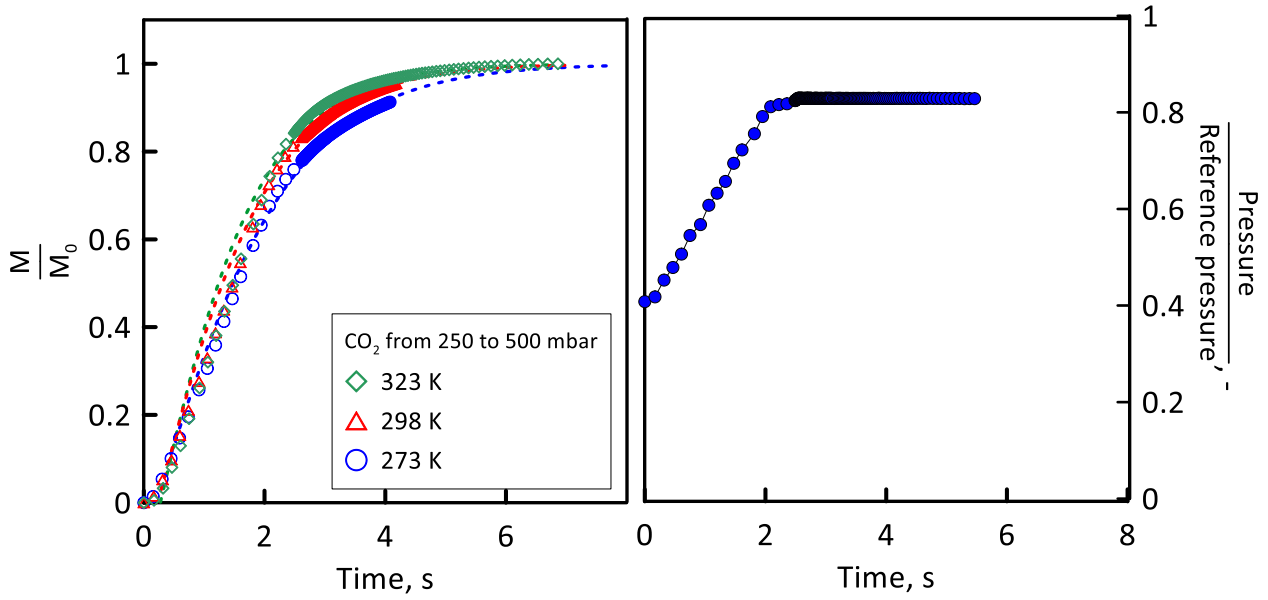

Fig. 3. (Left-side) Transient adsorption curve of single gas CO_2 adsorption on carbon hollow fiber membrane at 273 K (circles), 298 K (triangles) and 323 K (squares). Data regression with Eq. (5). (Right-side) Pressure "step" for transient adsorption curve. Reference pressure = 500 mbar.

Table 4
Permeability and gas selectivity measured at 308 K.

Feed composition (molar ratio)	Maximum feed pressure (bar)	Permeability (barrer)		CO_2/CH_4 selectivity
		CO_2	CH_4	
Single gas*	9	120.9 ± 1.76	2.3 ± 0.11	53.3 ± 4.7
Mixture 1	9.6	107.4 ± 1.90	1.04 ± 0.09	103.4 ± 6.7
		Permeability difference, %		Selectivity ratio, -
		11	54.7	1.9

3.2. Gas permeation performance

This activity focuses on the evaluation of the effect that H_2S and water vapor on the separation performance of the membranes, in the logic of understanding how these membranes can behave in presence of mixed gas streams much closer to industrial compositions. Single gas permeation measurements were first carried out to use this measure as a reference for quantifying the separation properties variations in presence of other gas species, such as a mixture, but also contaminants and water vapor. As mentioned, the objective is to use these membranes for biogas upgrading, therefore we measured the permeability of CO_2 and CH_4, as single gas. The obtained separation properties agreed with the main literature results obtained on analogous symmetric carbon hollow fiber membranes prepared starting from the same precursor (Table S3) [10,32-36]. The experimental data reveal that CO_2 was the most permeable gas (Table 4), confirming what was already reported in the literature [17,18,37], where the inverse proportionality of the permeability values with the kinetic diameter of molecules (CO_2: 3.3 Å, CH_4: 3.8 Å) is ascribed to a transport mechanism that is dominated by diffusion. These values were assumed as references for the first part of the experiments.

After single gas, a binary mixture with a composition (Mixture 1 - Table 1) typical of biogas main components (CO_2:CH_4 = 39.8:60.2) was fed to evaluate the membrane separation properties and the eventual mutual influence that gas could have on the permeation of the other one. CO_2 remained the most permeable gas. Both gases showed a lower permeability with respect to the single gas reference values, with a reduction of about 11% and 54.7% for CO_2 and CH_4, respectively. In literature, the permeation through the carbon membranes is mainly named as molecular sieving transport mechanism [17,18]; however, the reduction of the permeability of both gases observed in mixed conditions can be attributed to the competitive sorption of both gases during their permeation. Looking at the adsorption isotherms of the two gases on these membranes (Fig. 2), for a set temperature and pressure, CO_2 was the most adsorbed species followed by CH_4. Similarly, to what was observed in literature for zeolite membranes [38,39], in mixed gas conditions there could be a competition among the various gases in occupying the adsorption sites. In particular, CO_2 could preferentially occupy sorption sites in competition with CH_4. This could reflect a reduction of the permeability of both gases with respect to the correspondent single gas value, but much larger for CH_4, owing to the CO_2 preferential sorption, which corresponds to a higher CO_2/CH_4 selectivity.

3.3. Exposure to H_2S

As mentioned previously, long-term tests were carried out also to evaluate the separation properties of the membrane module in the presence of H_2S or water vapor, either as single compounds or in combination. The membrane module was continuously exposed to the gas stream; when no measurements were performed, the module was maintained at the reference operating condition (Table 1). This was done to guaranty the continuous exposition of the membrane to gases, since the aim of the work is to evaluate the separation properties also as a function of time in conditions closer to real ones, where the membranes are continuously under gas flow. After the experiments with the dry gas mixture (mixture 1, Table 1), the membrane module was exposed to an N_2 stream containing 462 ppm of H_2S, under a feed pressure of 9.6 bar (Fig. 4) for 3 days. Afterward, permeation measurements were continued by feeding a simulated biogas mixture (Mixture 2 in Table 1) containing 203 ppm of H_2S. The exposure of the membrane to the H_2S provoked a significant reduction of the permeability of 49 % and 64 % for CO_2 and CH_4, respectively with a consequent variation in selectivity, which was 1.4 times higher than single gas one (Fig. 5), but lower (75.4) with respect to the mixed gas without H_2S (98.7). The testing with the mixed gas containing H_2S lasted for around 4 h, afterward the performance of the membranes was evaluated by feeding a "clean" mixed gas stream not containing H_2S. Despite the absence of H_2S, the permeability of both gases remained constant in the new lower values, without recovering the performance shown before the exposure to the contaminant. Most likely, H_2S remained adsorbed in the membrane, reducing the availability of sorption sites to the other two gases.

For this purpose, a thermal treatment under N_2 flow at 363 K and 9.6 bar was performed in order to facilitate the removal of the H_2S eventually adsorbed in the membranes. The higher temperature was not possible to be applied due to the limitations imposed by the potting glue. After these 3 days treatment period, we observed a slight recovery of membrane performance with an increase of 11 and 7 % of CO_2 and CH_4 permeability, respectively corresponding to a CO_2 permeability of 69.6 barrer and a CH_4 permeability of 0.85 barrer (Fig. 4– top side). This reflected also on selectivity, which after treatment stood at a value of 82 (Fig. 4 – bottom side). However, we did not recover the initial membrane performance. It has to be noticed that adsorption onto activated carbon is a method used for cleaning biogas from contaminants such as

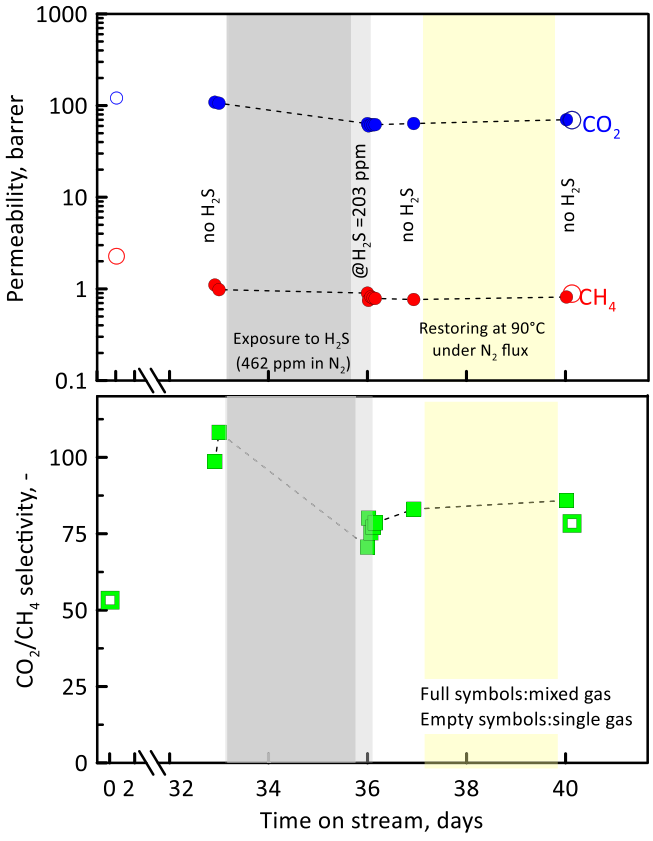

Fig. 4. CO_2 and CH_4 permeability (top-side); CO_2/CH_4 selectivity (bottom-side) as a function of time on stream at different feeding compositions.

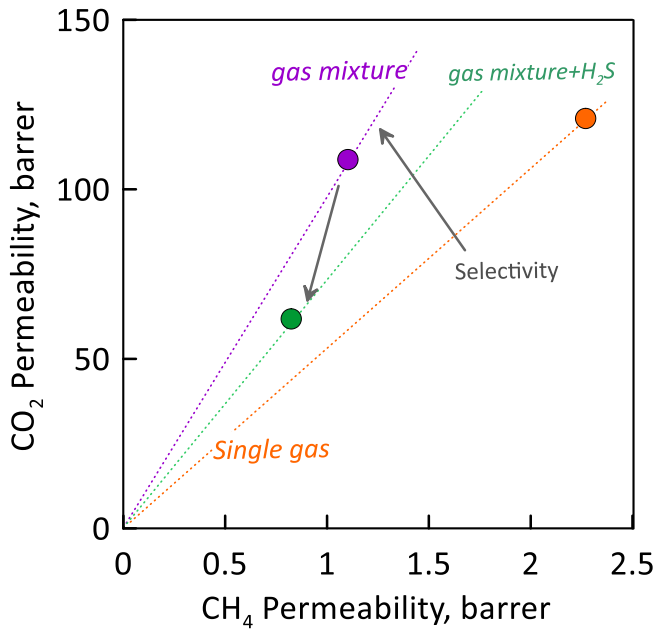

Fig. 5. CO_2 permeability as function of CH_4 permeability in single and mixed gas conditions, also in presence of H_2S. Experimental data (symbols).

H_2S. Therefore, besides the thermal treatment, it was not possible to remove all the adsorbed H_2S molecules from the membrane bulk. This behavior can be assimilated to that observed for zeolite membranes [39,40,40], where the presence of a gas strongly adsorbed into the membrane bulk can cause a loss of the availability of sorption sites to the permeation of other gases such as CO_2 and CH_4, whose sorption contribution to permeability remains relevant, but also a sort of hindering effect induced by the presence of H_2S molecules adsorbed on the pore walls, which reflects in a reduction of free pore volume available for diffusion.

3.4. Exposure to water vapor

After a stand-by period of 21 days, we evaluated the membrane performance in presence of water vapor (Fig. 6). Before starting these measurements, single gases confirmed no significant variations with respect to the results obtained before the stand-by period. The membrane module was continuously fed for 28 days with a CO_2 stream humidified at 90 % of relative humidity, at the reference operating conditions.

During this testing period the CO_2 permeability was measured continuously while the CH_4 permeability was only periodically checked. CH_4 permeability was not possible to be measured as it was below the detection limits of the setup (2 mmol m^{-2} s^{-1}) used for single gas measurements. Since the wet stream exposure was chronologically subsequent to the H_2S-containing stream exposition, the reference state for the calculation of the permeability differences was defined as the single gases permeabilities measured after the H_2S exposure.

The presence of water vapor in the feed stream provoked a significant reduction of CO_2 permeability, from a value of 69.5 barrer measured with single dry gas to 20.1 barrer, a value which was subsequently maintained relatively constant for the whole testing period of 28 days. The 71 % permeability reduction observed can be explained considering two different aspects. As it is well known [41,42], even if carbon surfaces are basically hydrophobic, when exposed to water vapor, the microporous walls of the carbon membranes are partially covered with an oxygen-containing functional group [12], which confers to the membrane a hydrophilic character. This can lead to two distinct phenomena: on one hand, strong competitive adsorption between the water vapor and CO_2 which reflects in a reduction of CO_2 permeability. On the other hand, as already observed also in polymeric and zeolite membranes [43,44], once the first layer of water molecules is adsorbed onto the pore walls, adsorbate–absorbate interactions can promote further adsorption of more water through hydrogen bonds, inducing the formation of clusters which can lead to a hindering effect to the permeation of the other gases, as well as to the reduction of the volume available for the diffusion of the gases through the membrane.

Dry single gas measurements were again performed after the membrane exposure to water vapor. The first measurement carried out with single CO_2 showed a permeability not significantly different than that measured with the humidified stream, which is probably attributed to the presence of residual water adsorbed/clustered in the membrane matrix. To favour water molecules removal, another thermal treatment that lasted 6 days, at 363 K at 9.6 bar under N_2 flow was carried out.

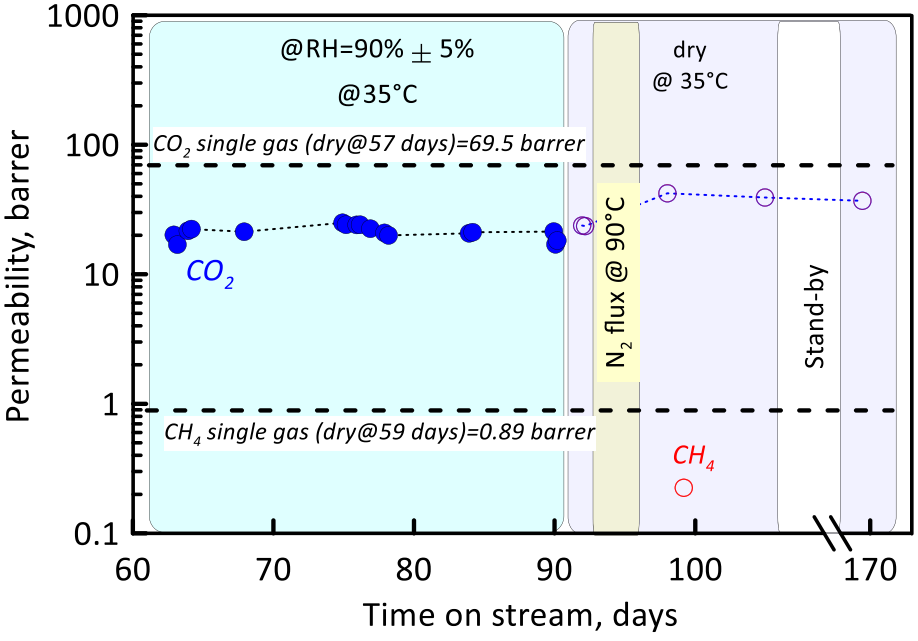

Fig. 6. CO_2 and CH_4 single gas permeability as a function of time on stream with dry and wet single gas.

After this treatment, we reduced the temperature to 308 K and evaluated the single dry gas permeabilities.

The permeability of CO_2 settled on an almost constant value of about 39.2 barrer, which was higher than the one measured before the thermal treatment, but remains lower than the one measured before starting the experiments with a humidified stream. Most likely, the thermal treatment was not sufficient to remove all the water molecules present in the matrix, reflecting in systematic reduction of the permeability of both gases (Fig. 6). After a stand-by period of 62 days, the CO_2 dry gas permeability was again checked and did not differ significantly from the one measured before, being 37 barrer against 39.2 barrer.

As observed in the literature [43], the exposure of the membranes to a continuous gas flow in a controlled environment can limit and, in some cases, avoid physical aging intended as narrowing of pores due to matrix shrinkage and/or pore-clogging due to dust and atmospheric moist. The CO_2 permeability in dry conditions was continuously monitored for another 15 days (Fig. 7). Overall, in the whole period, we observed a drop of 16 % passing from 37 to 31.1 barrer. After this, we evaluated the mixed gases in dry and wet conditions. Since the membrane did not recover its previous performances, as single gas reference values for this second round of experiments we considered the ones measured on the 181st day.

When CO_2 was mixed with CH_4 in dry conditions, we did not observe appreciable differences in permeability measured with single gas (Fig. 8 and Table S4). Analogously for CH_4 permeability, whose difference was about 2.4 %. Different behaviour was observed feeding the humid mixed gas stream. In this case, the CO_2 permeability was more than 30% lower than single gas, but also than the value measured in mixed gas dry conditions. This was the same behavior observed in Fig. 6 with CO_2 single gas humidified at RH = 90% and analogously can be attributed to the competitive permeation among the various gases present in the feed. Also, CH_4 permeability was reduced by more than a half, passing from 0.206 in dry mixed gases conditions to 0.096 barrer.

Fig. 9 summarizes the differences in separation properties at the different feeding conditions at the various experiments run-time. The permeabilities of both gases reduced during the time as a consequence of the different feeding conditions. CH_4 permeability was affected to a larger extent (Fig. 9, left-side), reflecting an increase of CO_2/CH_4 selectivity, which passed from 98.7 measured with dry mixed gas at 33 days to 149 after 182 days and then 217 in presence of water vapor in the feed. As depicted in Fig. 9 (right-side), when water vapor was present in the feed, the water molecules were adsorbed onto carbon matrix owing to the oxygenated active sites, which caused a competition on the sorption sites with both CO_2 and CH_4, and thus leading to the reduction of gas permeability [45,46]. However, it is worth noting that water vapor also permeates through the hydrophilic carbon membranes causing the coupled transport with CO_2, the overall influence is that the reduction in CO_2 permeability is not as significant as CH_4. As a result, the CO_2/CH_4 selectivity is enhanced in the wet mixed gas compared to dry mixed gas. When H_2S was fed into the feed stream, however, both the CO_2 permeability and CO_2/CH_4 selectivity were reduced. In particular,

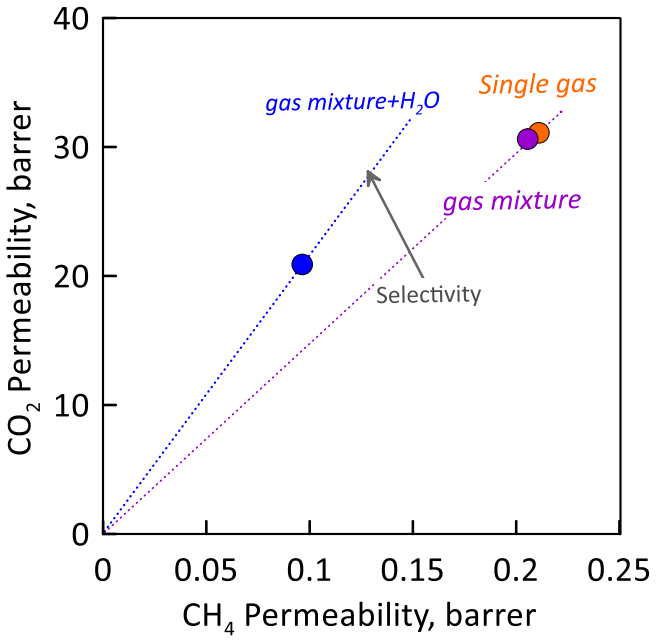

Fig. 8. CO_2 permeability as a function of CH_4 permeability in single gas (@181 day), mixed gas (@182 day), also in presence of relative humidity (@183 day). Experimental data (symbols).

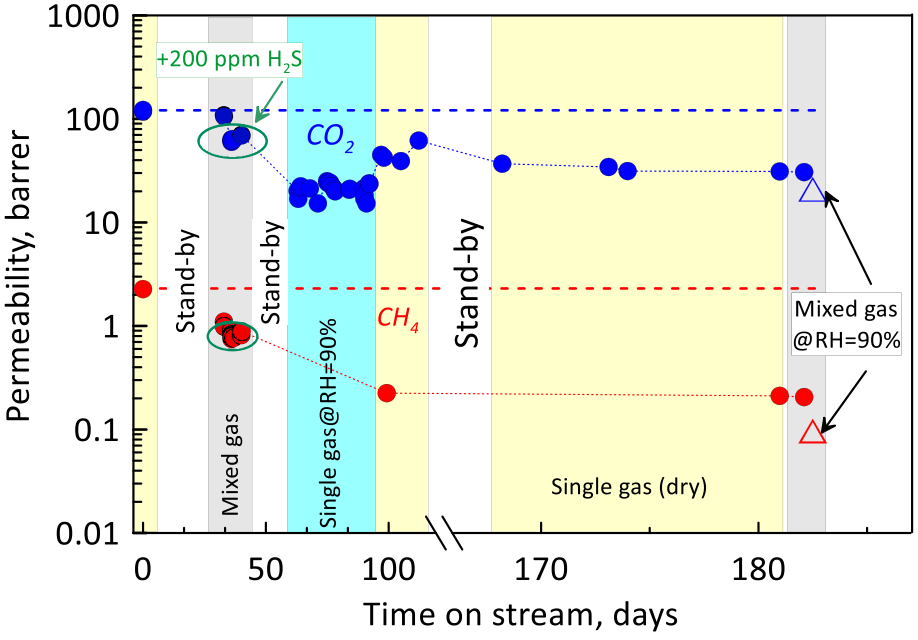

Fig. 7. CO_2 and CH_4 permeability as a function of time on stream at different feeding conditions. CO_2 (blue symbols), CH_4 (red symbols). Dashed lines correspond to single gas permeability at day 1.

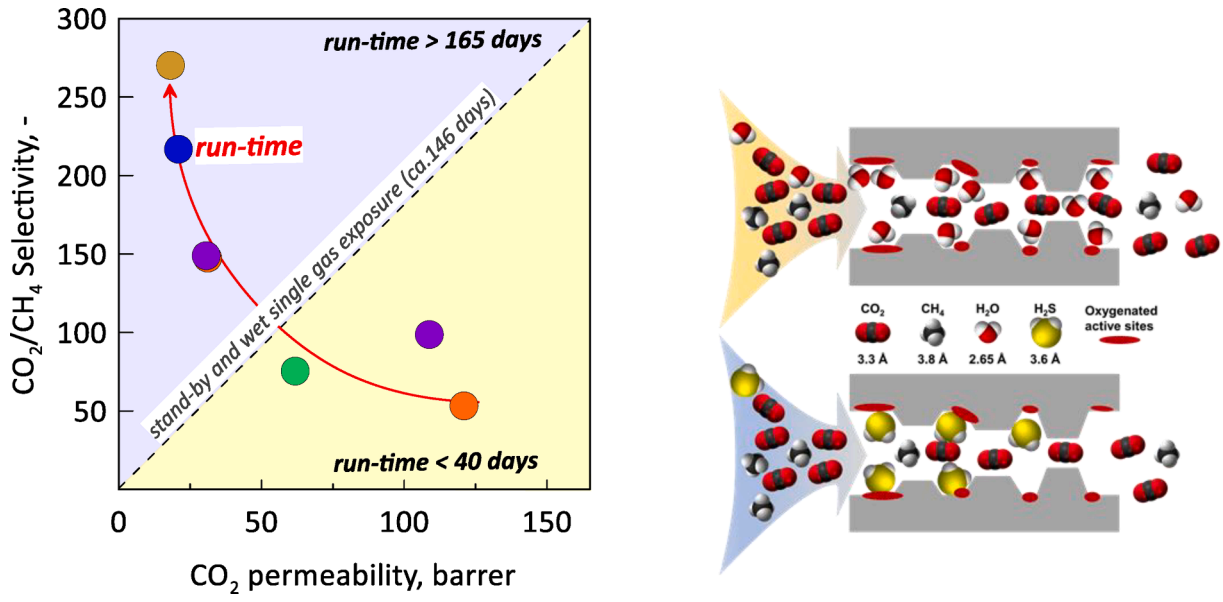

Fig. 9. CO_2/CH_4 selectivity as a function of CO_2 permeability at different feeding conditions. Single gas (orange symbols), Dry mixed gas + H_2S (green symbol), dry mixed gas (violet symbols), wet mixed gas (blues symbol), wet mixed gas + H_2S (gold symbol) (left-side); The selective permeation mechanisms for the membranes under a humidified condition (right-top) and H_2S exposure (Right-bottom).

the exposure to the H_2S reduced CO_2 and CH_4 permeability by 43.2% and 25.3%, respectively, compared to the mixed gas feeding without H_2S, with a selectivity drop of about 23.5%. This is caused by the strong adsorption of H_2S molecules that hindered both CO_2 and CH_4 adsorption on the carbon matrix. Besides, owing to the larger kinetic diameter of H_2S (3.6 Å) than water (2.65 Å), the adsorbed H_2S molecules created a more significant resistance to CO_2 and CH_4 transport, compared to the adsorbed water molecules. More importantly, we exclude any relevant effect owed to physical aging since the drop of performance observed with H_2S-containing mixture occurred in less than 3 days from the last measurements with dry mixed gases (velvet symbol – Fig. 9) and also because during the stand-by periods the membranes are kept under controlled environment with a continuous N_2 flow. The second half of the graph (violet portion– Fig. 9), refers to the experiments carried out after 180 days of testing. As highlighted in the figures above, in this range we included a stand-by period (27 days) followed by long-term testing with humidified CO_2 (28 days), then another stand-by of 62 days. As aforementioned, the measurements carried out with humidified CO_2 evidenced a reduction of permeability mainly attributed to water presence in the feed; after this test, the permeability reduction registered in dry mixed gas conditions was not so significant, and in any case less relevant than that observed in the first phase of experiments (yellow portion of– Fig. 9), as confirmed by the overlap of the violet point (dry mixed gas @182 day) on the orange one (single gas @181 day) in the violet portion of– Fig. 9.

Comparing the two experiments carried out with dry mixed gases at the two different timing (violet symbols – Fig. 9), the fact that the membrane underwent the presence of water vapor and H_2S induced an overall advantage in terms of selectivity (+51%), whereas a significant loss of CO_2 permeability (−72%). As expected, in wet mixed gas conditions, the water vapor presence affected much more the less permeable gas, with a consequent higher selectivity.

Overall, the membranes underwent 183 days of continuous testing, without being damaged or losing their capability to separate CO_2/CH_4 stream. As further confirmation, we stored the membranes for 181 days (without any exposure to gas), after which we repeated some measurements. After the exposure under N_2 flow at 363 K and 9.6 bar lasted 24 h, the membrane showed a CO_2 single gas permeability of 38.6 barrer (at 308 K), close to the one measured at day 181st (31.1 barrer), after the continuous testing. This indicated that no physical aging occurred during the storing period and that the results can be compared as there is no influence related to the time gap. Afterwards, a mixture containing both H_2S and water vapour (Mixture 2 at RH = 90%) was fed to the membrane module to analyze the eventual synergic effect of the two species on the separation performance. CO_2 permeability reduced of about 49% with respect to the single gas measured the day before, and the CO_2/CH_4 selectivity was close to 270 (Table S5) (gold symbol – Fig. 9). Comparing these measurements with the results obtained feeding wet mixed gas but without H_2S (day 183rd), we noticed an additional reduction of permeability of both gases that can be ascribed to H_2S presence (18.1 barrer and 0.067 barrer against 20.9 barrer and 0.096 for CO_2 and CH_4, respectively) and which reflected in a further increment of CO_2/CH_4 selectivity, which passed from 217 to 270, analogously to what we observed feeding the dry mixture containing 203 ppm of H_2S. Therefore, we can conclude that when H_2S and water vapour are contemporary present in a mixture, their synergic effect induces a significant reduction of gas permeabilities with consequent increment of selectivity.

4. Conclusions

In this work, we investigated, for 183 days of continuous exposure, the long-term performance of as-prepared cellulose-based carbon hollow fiber membranes in the separation of simulated biogas mixtures, also in presence of H_2S (up to 500 ppm) and water vapor (RH = 90%).

The sorption isotherms showed a higher affinity of the membrane material to CO_2, which dominated the sorption in the membrane matrix, resulting in a CO_2 concentration three times higher than that of CH_4. However, the analysis of results showed a limited contribution of sorption to selectivity, confirming that the permeation through the membrane is mainly controlled by diffusion.

It was found that the exposure of the membrane module to the H_2S provoked a reduction of both the CO_2 and CH_4 permeability by 43% and 25%, respectively, compared to the mixed gas feeding without H_2S, with a drop in selectivity of about 23%. This was caused by the strongly adsorbed effect of H_2S molecules onto the carbon matrix surface or into the micropores, leading to a loss of the availability of the sorption site to the permeation gases of CO_2 and CH_4.

The exposure to humidified gas streams soon caused a CO_2 permeability reduction of about 67%, mostly ascribable to strong competitive

adsorption between the water vapor and CO_2 as well as to water molecules clustering in the membrane pores. Then, the separation performance of the membrane module remained relatively constant with a CO_2/CH_4 selectivity of more than 200 at 28 days of continuous testing.

Overall, the membranes underwent more than 183 days of continuous testing, and were tested for a whole period of 364 days, also in presence of contaminants and water vapor, without being damaged or losing their capability to separate CO_2/CH_4 stream, thus confirming to be attractive candidates for their application in biogas upgrading.

Declaration of Competing Interest

The authors declare that they have no known competing financial interests or personal relationships that could have appeared to influence the work reported in this paper.

Acknowledgements

The authors A. Brunetti, G. Barbieri acknowledge the project BIOVALUE "Advanced Membranes for biogas upgrading and high added-value compounds recovery", co-funded by Regione Calabria in the framework of M-Era.Net 2018 is for co-funding this work. A. Brunetti and E. P. Favvas acknowledge the National Research Council of Italy in the framework of the Short-Term Mobility program 2021 for co-funding this work. The authors L. Lei, A. Lindbråthen, E. P. Favvas and X. He acknowledge the CO2Hing project from the Research Council of Norway.

Appendix A. Supplementary data

Supplementary data to this article can be found online at https://doi.org/10.1016/j.cej.2022.137615.

References

[1] Net Zero by 2050, in, International Energy Agency, Paris, 2021 (last access: 07-03-2022).
[2] C.Y. Chuah, K. Goh, Y. Yang, H. Gong, W. Li, H.E. Karahan, M.D. Guiver, R. Wang, T.-H. Bae, Harnessing filler materials for enhancing biogas separation membranes, Chem. Rev. 118 (2018) 8655–8769, https://doi.org/10.1021/acs.chemrev.8b00091.
[3] J.H. Ebner, R.A. Labatut, M.J. Rankin, J.L. Pronto, C.A. Gooch, A.A. Williamson, T. A. Trabold, Lifecycle greenhouse gas analysis of an anaerobic codigestion facility processing dairy manure and industrial food waste, Environ. Sci. Technol. 49 (2015) 11199–11208, https://doi.org/10.1021/acs.est.5b01331.
[4] A. Brunetti, G. Barbieri, Membrane engineering for biogas valorization, perspective, Front. Chem. Eng. 3 (2021) 775–788, https://doi.org/10.3389/fceng.2021.775788.
[5] R.W. Baker, K. Lokhandwala, Natural gas processing with membranes: an overview, Ind. Eng. Chem. Res. 47 (2008) 2109–2121, https://doi.org/10.1021/ie071083w.
[6] L.M. Robeson, The upper bound revisited, J. Mem. Sci. 320 (2008) 390–400, https://doi.org/10.1016/j.memsci.2008.04.030.
[7] M.-B. Hägg, J.A. Lie, A. LindbrÅThen, Carbon molecular sieve membranes, Ann. Ny. Acad. Sci. 984 (2003) 329–345.
[8] X. He, M.-B. Hägg, Membranes for environmentally friendly energy processes, Membranes 2 (4) (2012) 706–726.
[9] X.Y. Chen, H. Vinh-Thang, A.A. Ramirez, D. Rodrigue, S. Kaliaguine, Membrane gas separation technologies for biogas upgrading, RSC Adv. 5 (2015) 24399–24448, https://doi.org/10.1039/C5RA00666J.
[10] L. Lei, L. Bai, A. Lindbråthen, F. Pan, X. Zhang, X. He, Carbon membranes for CO_2 removal: Status and perspectives from materials to processes, Chem. Eng. J. 401 (2020), 126084, https://doi.org/10.1016/j.cej.2020.126084.
[11] S. Haider, A. Lindbråthen, J.A. Lie, P.V. Carstensen, T. Johannessen, M.-B. Hägg, Vehicle fuel from biogas with carbon membranes; a comparison between simulation predictions and actual field demonstration, Green Energy Environ. 3 (2018) 266–276, https://doi.org/10.1016/j.gee.2018.03.003.
[12] S. Haider, A. Lindbråthen, J.A. Lie, M.-B. Hägg, Regenerated cellulose based carbon membranes for CO_2 separation: durability and aging under miscellaneous environments, J. Ind. Eng. Chem. 70 (2019) 363–371, https://doi.org/10.1016/j.jiec.2018.10.037.
[13] D.S. Karousos, L. Lei, A. Lindbråthen, A.A. Sapalidis, E.P. Kouvelos, X. He, E. P. Favvas, Cellulose-based carbon hollow fiber membranes for high-pressure mixed gas separations of CO_2/CH_4 and CO_2/N_2, Sep. Purif. Technol. 253 (2020), 117473, https://doi.org/10.1016/j.seppur.2020.117473.
[14] S.C. Rodrigues, M. Andrade, J. Moffat, F.D. Magalhães, A. Mendes, Preparation of carbon molecular sieve membranes from an optimized ionic liquid-regenerated cellulose precursor, J. Membr. Sci. 572 (2019) 390–400, https://doi.org/10.1016/j.memsci.2018.11.027.
[15] L. Lei, F. Pan, A. Lindbråthen, X. Zhang, M. Hillestad, Y. Nie, L. Bai, X. He, M. D. Guiver, Carbon hollow fiber membranes for a molecular sieve with precise-cutoff ultramicropores for superior hydrogen separation, Nat. Commun. 12 (2021) 268, https://doi.org/10.1038/s41467-020-20628-9.
[16] L. Lei, A. Lindbråthen, M. Hillestad, X. He, Carbon molecular sieve membranes for hydrogen purification from a steam methane reforming process, J. Membr. Sci. 627 (2021), 119241, https://doi.org/10.1016/j.memsci.2021.119241.
[17] L. Lei, A. Lindbråthen, M. Hillestad, M. Sandru, E.P. Favvas, X. He, Screening cellulose spinning parameters for fabrication of novel carbon hollow fiber membranes for gas separation, Ind. Eng. Chem. Res. 58 (2019) 13330–13339, https://doi.org/10.1021/acs.iecr.9b02480.
[18] L. Lei, A. Lindbråthen, X. Zhang, E.P. Favvas, M. Sandru, M. Hillestad, X. He, Preparation of carbon molecular sieve membranes with remarkable CO_2/CH_4 selectivity for high-pressure natural gas sweetening, J. Membr. Sci. 614 (2020), 118529, https://doi.org/10.1016/j.memsci.2020.118529.
[19] E.P. Favvas, E.P. Kouvelos, S.K. Papageorgiou, C.G. Tsanaktsidis, A.C. Mitropoulos, Characterization of natural resin materials using water adsorption and various advanced techniques, Appl. Phys. A 119 (2015) 735–743, https://doi.org/10.1007/s00339-015-9022-6.
[20] M.A. Al-Ghouti, D.A. Daana, Guidelines for the use and interpretation of adsorption isotherm models: a review, J. Hazard. Mater. 393 (2020), 122383, https://doi.org/10.1016/j.jhazmat.2020.122383.
[21] J. Crank, The mathematics of diffusion, 2nd Edition, Brunel University, Uxbridge, Clarendon Press Oxford, 1975, ISBN 0198533446.
[22] B. Liu, Y. Li, L. Hou, G. Yang, Y.-Y. Wang, Q.-Z. Shi, Dynamic Zn-based metal–organic framework: stepwise adsorption, hysteretic desorption and selective carbon dioxide uptake, J. Mater. Chem. A 1 (2013) 6535–6538, https://doi.org/10.1039/C3TA10918F.
[23] R.P.P.L. Ribeiro, I.A.A.C. Esteves, J.P.B. Mota, Adsorption of carbon dioxide, methane, and nitrogen on Zn(dcpa) metal-organic framework, Energies 14 (2021) 5598, https://doi.org/10.3390/en14185598.
[24] E.P. Favvas, G.E. Romanos, S.K. Papageorgiou, F.K. Katsaros, A.C. Mitropoulos, N. K. Kanellopoulos, A methodology for the morphological and physicochemical characterisation of asymmetric carbon hollow fiber membranes, J. Membr. Sci. 375 (2011) 113–123, https://doi.org/10.1016/j.memsci.2011.03.028.
[25] M.B. Rao, S. Sircar, Nanoporous carbon membranes for separation of gas mixtures by selective surface flow, J. Membr. Sci. 85 (1993) 253–264, https://doi.org/10.1016/0376-7388(93)85279-6.
[26] E.P. Favvas, E.P. Kouvelos, G.E. Romanos, G.I. Pilatos, A. Ch, Mitropoulos and N. K. Kanellopoulos,, Characterization of highly selective microporous carbon hollow fiber membranes prepared from a commercial co-polyimide precursor, J. Porous Materials 15 (2008) 625–633, https://doi.org/10.1007/s10934-007-9142-2.
[27] N. Kruse, Y. Schießer, N. Reger-Wagner, H. Richter, I. Voigt, G. Braun, J.-U. Repke, High pressure adsorption, permeation and swelling of carbon membranes – Measurements and modelling at up to 20MPa, J. Membr. Sci. 544 (2017) 12–17, https://doi.org/10.1016/j.memsci.2017.09.004.
[28] O. Sanyal, C. Zhang, G.B. Wenz, S. Fu, N. Bhuwania, L. Xu, M. Rungta, W.J. Koros, Next generation membranes–using tailored carbon, Carbon 127 (2018) 688–698, https://doi.org/10.1016/j.carbon.2017.11.031.
[29] F. Rouquerol, J. Rouquerol, K.S.W. Sing, P. Llewellyn and G. Maurin (Eds), Adsorption by Powders and Porous Solids Principles, Methodology and Applications, 2nd edition, Kidlington, Oxford OX5 1GB, UK (2014) ISBN: 9780080970356.
[30] S. Fu, G.B. Wenz, E.S. Sanders, S.S. Kulkarni, W. Qiu, C. Ma, W.J. Koros, Effects of pyrolysis conditions on gas separation properties of 6FDA/DETDA:DABA(3:2) derived carbon molecular sieve membranes, J. Membr. Sci. 520 (2016) 699–711, https://doi.org/10.1016/j.memsci.2016.08.013.
[31] M. Balsamo, F. Rodríguez-Reinoso, F. Montagnaro, A. Lancia, A. Erto, Highlighting the role of activated carbon particle size on CO_2 capture from model flue gas, Ind. Eng. Chem. Res. 52 (2013) 12183–12191, https://doi.org/10.1021/ie4018034.
[32] X. He, M.-B. Hägg, Hollow fiber carbon membranes: from material to application, Chem. Eng. J. 215–216 (2013) 440–448, https://doi.org/10.1016/j.cej.2012.10.051.
[33] X. He, M.-B. Hägg, Structural, kinetic and performance characterization of hollow fiber carbon membranes, J. Membr. Sci. 390–391 (2012) 23–31, https://doi.org/10.1016/j.memsci.2011.10.052.
[34] C. Zhang, W.J. Koros, Ultraselective carbon molecular sieve membranes with tailored synergistic sorption selective properties, Adv. Mater. 29 (2017) 1701631, https://doi.org/10.1002/adma.201701631.
[35] M. Yoshimune, I. Fujiwara, K. Haraya, Carbon molecular sieve membranes derived from trimethylsilyl substituted poly(phenylene oxide) for gas separation, Carbon 45 (2007) 553–560, https://doi.org/10.1016/j.carbon.2006.10.017.
[36] M. Yoshimune, K. Haraya, Simple control of the pore structures and gas separation performances of carbon hollow fiber membranes by chemical vapor deposition of propylene, Sep. Purif. Technol. 223 (2019) 162–167, https://doi.org/10.1016/j.seppur.2019.04.065.
[37] P.H.T. Ngamou, M.E. Ivanova, O. Guillon, W.A. Meulenberg, High-performance carbon molecular sieve membranes for hydrogen purification and pervaporation dehydration of organic solvents, J. Mater. Chem. A 7 (12) (2019) 7082–7091.
[38] P.F. Zito, A. Caravella, A. Brunetti, E. Drioli, G. Barbieri, Discrimination among gas translation, surface and Knudsen diffusion in permeation through zeolite

membranes, J. Membr. Sci. 564 (2018) 166, https://doi.org/10.1016/j.memsci.2018.07.023.
[39] P.F. Zito, A. Brunetti, A. Caravella, E. Drioli, G. Barbieri, Mutual influence in permeation of CO_2-containing mixtures through a SAPO-34 membrane, J. Membr. Sci. 595 (2020), 117534, https://doi.org/10.1016/j.memsci.2019.117534.
[40] P.F. Zito, A. Caravella, A. Brunetti, E. Drioli, G. Barbieri, Knudsen and surface diffusion competing for gas permeation inside silicalite membranes, J. Membr. Sci. 523 (1) (2017) 456–469, https://doi.org/10.1016/j.memsci.2016.10.016.
[41] I. Menendez, A.B. Fuertes, Aging of carbon membranes under different environments, Carbon 39 (5) (2001) 733–740, https://doi.org/10.1016/S0008-6223(00)00188-3.
[42] C.J. Anderson, W. Tao, C.A. Scholes, G.W. Stevens, S.E. Kentish, The performance of carbon membranes in the presence of condensable and non-condensable impurities, J. Membr. Sci. 378 (1) (2011) 117, https://doi.org/10.1016/j.memsci.2011.04.058.
[43] A. Brunetti, M. Cersosimo, G. Dong, K.T. Woo, J. Lee, J.S. Kim, Y.M. Lee, E. Drioli, G. Barbieri, In situ restoring of aged thermally rearranged gas separation membranes, J. Membr. Sci. 520 (2016) 671–678.
[44] P.F. Zito, A. Brunetti, A. Caravella, E. Drioli, G. Barbieri, Water vapor permeation and its influence on gases through a zeolite-4A membrane, J. Membr. Sci. 574 (2019) 154–163, https://doi.org/10.1016/j.memsci.2018.12.065.
[45] T. Araújo, G. Bernardo, A. Mendes, Cellulose-based carbon molecular sieve membranes for gas separation: a review, Molecules 25 (2020) 3532–3565, https://doi.org/10.3390/molecules25153532.
[46] M.C. Campo, S. Lagorsse, F.D. Magalhães, A. Mendes, Comparative study between a CMS membrane and a CMS adsorbent: part II. Water vapor adsorption and surface chemistry, J. Membr. Sci. 346 (1) (2010) 26–36, https://doi.org/10.1016/j.memsci.2009.09.004.